Resonant Tunnel Diode (RTD) Stability

J. E. Morris and D. W. Matson
Department of Electrical & Computer Engineering, Portland State University
Portland, Oregon 97207-0751, U. S. A.
j.e.morris@ieee.org

***Abstract**: Small signal RTD behavior defines whether circuit applications will be stable or unstable. The paper presents a MATLAB analysis of a 3rd-order model to delineate graphical stability regions, and to interpret these with the assistance of prior 2nd-order results for Esaki tunnel diodes (TDs.) A new 4th-order model is developed, which is more successful in predicting published bias stability data.*

1. INTRODUCTION

RTDs offer the potential for terahertz operation in monolithic circuits where all functional units can be contained within regions of dimensions 20μm or so. The circuit concepts parallel those of Esaki TD circuits of the 1960's, with the same isolation problems of a two-terminal device. The need for three-terminal operation has led to a number of composite device configurations. However, the basic RTD is still the core device, and its circuit operation must be fully understood for successful design.

In particular, the question of bias stability is addressed in this paper, with application also to the transient switching behavior of the TD circuit as the switching transient approaches its final target bias point.

The basic principle of the RTD is illustrated in Figure 1. The device shown consists of two degenerate n-type semiconductors (e.g. n^+-GaAs) separated from a (GaAs) quantum well by two tunneling barriers of (ideally) equal thickness (e.g. $Al_xGa_{1-x}As$.) Well widths of 7nm and barrier thicknesses around 2.5nm are often quoted. Electrons in the well are restricted to narrow permitted energy levels, (e.g. E_1 in Figure 1,) and "resonant" tunneling through the double barrier takes place when the bias voltage aligns E_1 with the Fermi level in the supply electrode. As the voltage continues to increase, E_1 drops below the conduction band edge, and the resonant tunneling current falls off. One can observe multiple peaks if the tunneling barrier heights are sufficient for the quantum well to sustain multiple permitted levels. However, only a single peak is considered below. The excess current observed at higher bias comes from a mixture of normal two-step tunneling and thermionic emission over the barrier.

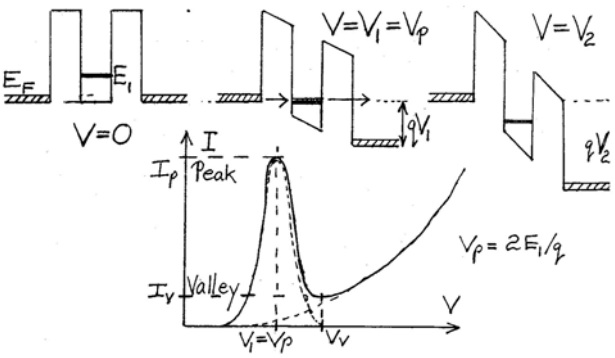

Fig. 1. Basic RTD concepts: energy band model and characteristics.

Three examples of practical characteristics are shown in Figure 2, reproduced from Reference [1]. Note the distortion observed in the negative resistance region of the RTD peak for the two higher current cases. This effect is well-known for TD curve-tracing, and comes from self-rectification (by the non-linear characteristic) of a parasitic high-frequency self-oscillation signal due to an unstable bias configuration as the characteristic sweep moves through the

negative resistance region. Note that this problem is not seen in the third case, where the current peak is lower, and the negative resistance slope less.

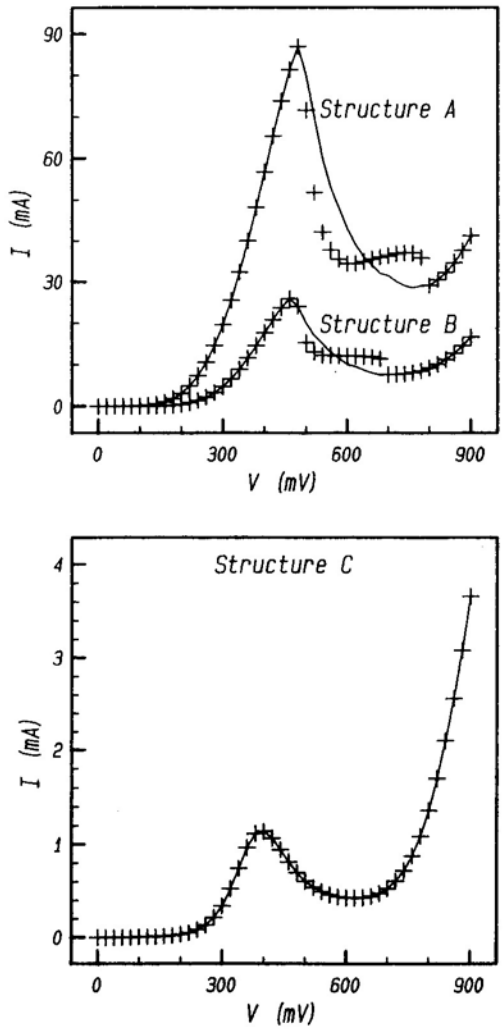

Fig. 2. Experimental RTD characteristics [1].

2. THEORY

A generic (bias) circuit is shown in Figure 3 [2], where the static RTD characteristic is represented by $I_j = f(V_j)$. A successful curve tracing of the static characteristic requires single intersections of the load line with the characteristic, i.e. a Thevenin voltage source impedance R less than the minimum negative differential resistance (NDR), $R_D = (dI_j/dV_j)^{-1}$. The resistances R_S and R_L are intended to represent non-ideal series, (bulk semiconductor, and interconnect or lead,) and load/source resistances, respectively. L_L similarly represents parasitic inductive effects.

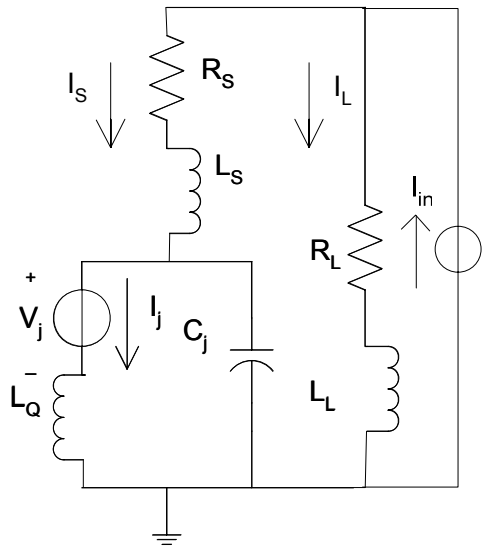

Fig. 3. Bias circuit for theoretical development.

The device capacitance, C_j, represents the sum of the depletion layer and "quantum" capacitances, C_d and $C_w=dQ_w/dV_j$, respectively, the latter associated with charge storage in the quantum well. C_j is clearly bias dependent, but is represented below as constant, C, for simplicity. It is also recognized that the quantum well electronic charge in the permitted energy level(s), which is required for the resonant tunneling mechanism, takes a finite time to establish by conventional single barrier tunneling. This effect can be represented by a "pseudo-inductance," but there is argument on where this should appear in the circuit model, i.e. as L_S [1] or L_Q [3]. (L_S includes parasitic lead inductance, and so might also be included in a circuit model with L_Q.)

The circuit equations may be solved by writing them in differential form, (with $dI_{in}/dt = 0$,) and translating the origin to the DC bias point, etc., or (more simply) by considering the small signal response in terms of $s=\sigma+j\omega$ in the complex plane.

2.1. Gering et al (L_S) Model [1]

Setting $L_Q = 0$ in Figure 3, gives the second-order characteristic equation:

$$s^2 + Ps + Q = 0,$$

where

$$P = R/L + 1/R_DC$$
$$Q = (1 + R/R_D)/LC$$

with $R=R_L+R_S$ and $L=L_L+L_S$. Note that the quantum pseudo-inductance is included within L_S in this case, (and may account for all of L_S.)

These results are the same as have been previously obtained for Esaki TD circuits, with interpretations as given below [4].

2.2. General (L_Q & L_S) Model (Fig. 3)

The general result for Figure 3 is a third-order characteristic equation:

$$s^3 + Ps^2 + Qs + T = 0,$$

where

$$P = R/L + R_D/L_Q$$
$$Q = (L + L_Q + RR_DC)/LL_QC$$
$$T = (R + R_D)/LL_QC$$

with $R=R_L+R_S$ and $L=L_L+L_S$, again.

2.3. Brown et al (L_Q) Model [3]

Setting $L_S = 0$ in Figure 3 gives the same result as in Section 2.2 immediately above, except with $L = L_L$.

2.4. New "Split-C" Composite L_Q Model

It does not seem reasonable that the quantum pseudo-inductance L_Q would control the development of the depletion region charge, so it should not be in series with C_D, but it equally clearly should be in series with C_W. Consequently, an alternative model is proposed for the next stage of work, with C split into its constituent parts. The modified model is shown in Figure 4. The characteristic equation of the generalized circuit with this model is a quartic:

$$s^4 + Ps^3 + Qs^2 + Ts + W = 0$$

where

$$P = R/L + 1/R_DC_W$$
$$Q = 1/L_QC_S + (1/C_D + R/R_DC_W)/L$$
$$T = ((L + L_Q)/RR_DC_W + R/C_S)/LL_Q$$
$$W = (1 + R/R_D)/LL_QC_DC_W$$

and $1/C_S = 1/C_D + 1/C_W$.

This can be reduced to a more manageable third order equation for L=0,

$$s^3 + Ps^2 + Qs + T = 0,$$

where

$$P = 1/R_DC_W + 1/RC_D$$
$$Q = 1/L_QC_S + 1/RR_DC_DC_W$$
$$T = C_DC_WL_Q/R_P$$

and $R_P = RR_D/(R+R_D)$.

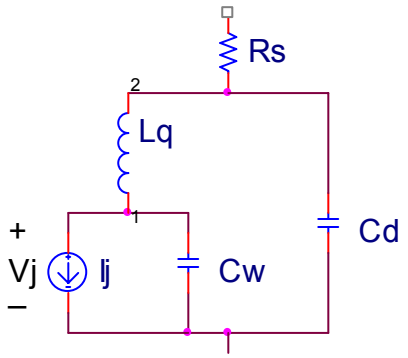

Fig. 4. Modified RTD model.

3. 2ND ORDER (GERING) MODEL

All possible circuit responses are classified by regions of the P-Q plane in Figure 5, with the corresponding roots, s_1 and s_2, of the characteristic equations illustrated for each region. The region Q<0 is only accessible for $R_D<0$ and $R>|R_D|$, and the complex plane response corresponds to a "saddle point." Stable bias requires P>0, which is achieved for all positive R_D, or with $R>L/|R_D|C$ for $R_D<0$. The parabola divides "node" and "focus" behaviors in regions where $Q>¼P^2$ and $Q<¼P^2$, respectively, and corresponds to the critical damping condition.

The forms of these (dynamic) behaviors are shown in Figure 6 for an instantaneous operating point in the vicinity of a bias point intersection of the DC (static) load line with the device characteristic.

An example of the variation of circuit responses as R_D varies with different TD bias points is shown in Figure 7 for nine different external circuits.

Focusing on Figures 5 and 6, one can see that a switching trajectory will settle to a stable bias point with an over-damped or under-damped response if the bias point is a stable node or stable focus respectively. One of these cases will apply for ALL regions of positive R_D slope. The situation is more interesting for the NDR region, for there is no real bias point for $R>|R_D|$, and saddle behavior prevails. In order to have a single-valued bias point in the NDR, it is necessary that $R<|R_D|$, and only the R=10Ω case in Figure 7 qualifies throughout the NDR region with $|R_D|_{MIN}$ = 25Ω. However, for the parameters given and L_{MIN}=10nH, R must be greater than 20Ω for stable curve-tracing at $|R_D|_{MIN}$, so the stable focus goes unstable around this region. In general, the unstable node situation corresponds to large L, and astable

multivibrator operation, whereas an unstable focus is usually observed as oscillation about the bias point, or as in Figure 2A&B, due to self-rectification.

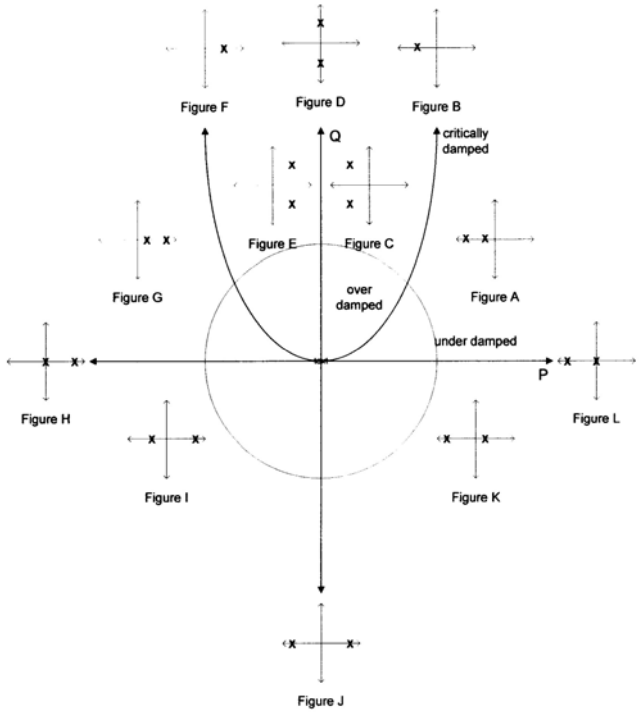

Fig. 5. 2nd order complex s-plane responses, and relationships to P-Q plane regions.

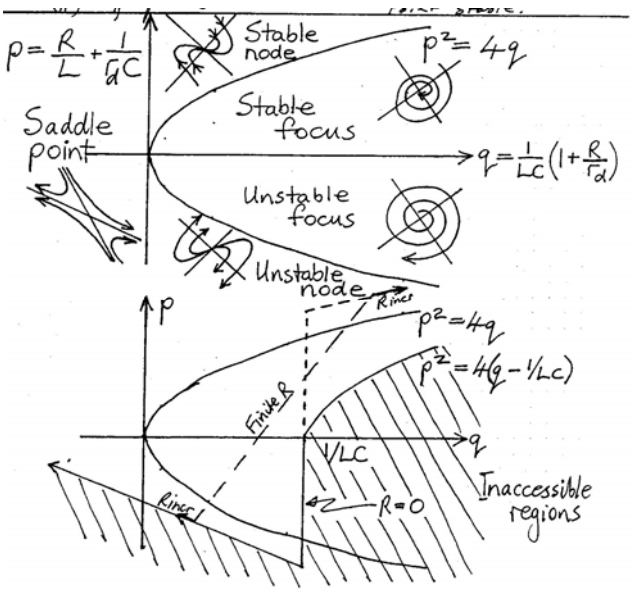

Fig. 6. 2nd order responses in the P-Q plane, and accessible regions for real circuits.

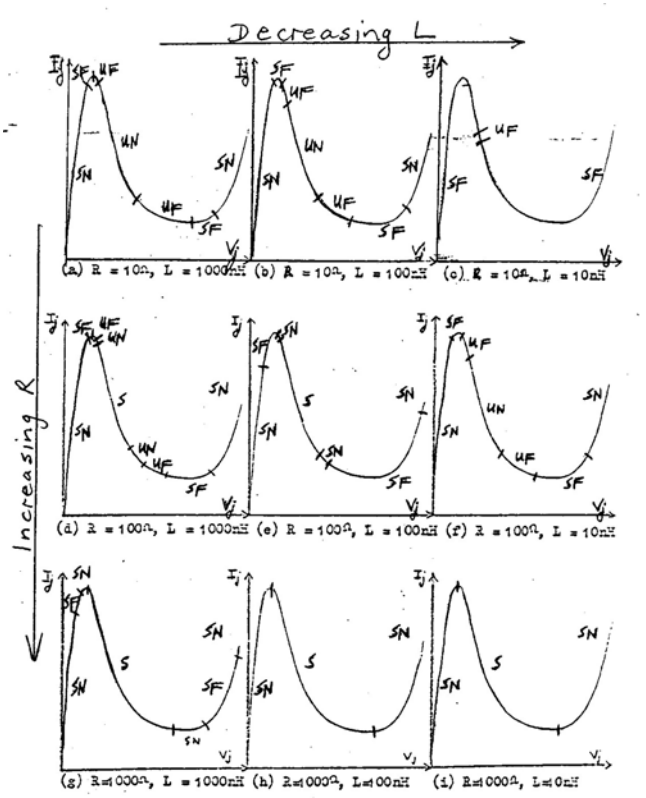

Fig. 7. Tunnel diode stability regions for R=10, 100, & 1000Ω, and L=10, 100, & 1000nH.
(TD: I_P = 5mA, I_V = 1mA, V_P = 60mV, V_V = 340mV; NDR $|R_D|_{MIN}$ = 25Ω; C = 20pF.)
S: saddle point; SN: stable node; SF: stable focus; UN: unstable node; UF: unstable focus.

4. 3RD ORDER (BROWN) MODEL

One of the objectives of this work has been to develop a 3-D equivalent of the 2-D P-Q plane diagram to similarly clarify the way in which stability and circuit performance vary with external circuit parameters and bias point on the device characteristic. Figures 8 and 9 show progress to date. The 3-D surfaces of Figure 9 are obviously not as easy to interpret as their 2-D equivalents, and only the T>0 case is shown. Figure 8 shows the s-plane responses, which are the same as for the 2nd order case, but with the addition of a stable left-hand half-plane root on the real axis. T<0 transfers this root to the unstable right-hand half-plane, whenever $R+R_D<0$, i.e. always when $R < |R_D|$ in the NDR region, i.e. for any DC bias configuration for NDR region curve-tracing. This would certainly seem to explain why there are almost no satisfactory RTD characteristic curves seen in the literature, (but note Figure 2C as an exception.)

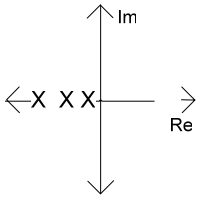

Fig. 8 W (stable node)

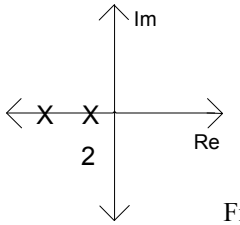

Fig. 8 WX

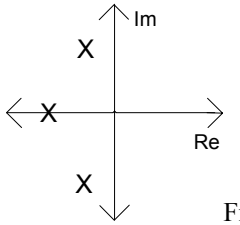

Fig. 8 X (stable focus)

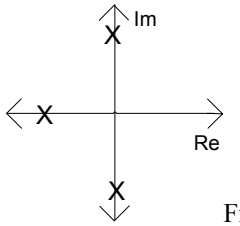

Fig. 8 XY

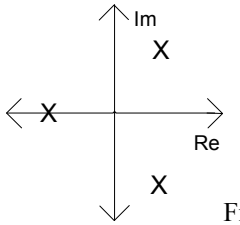

Fig. 8 Y (unstable focus)

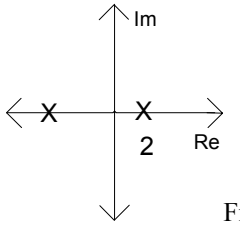

Fig. 8 YZ

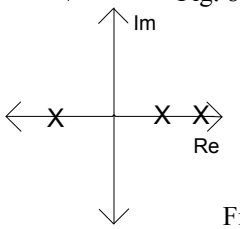

Fig. 8 Z (unstable node)

Fig. 8: Complex plane poles for transient responses.

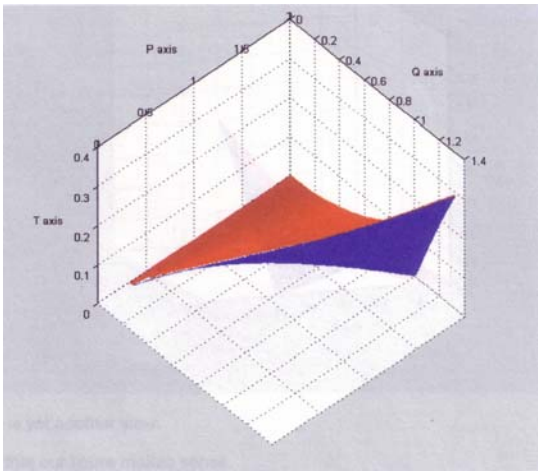

(a) Surface corresponds to Fig. 8: WX

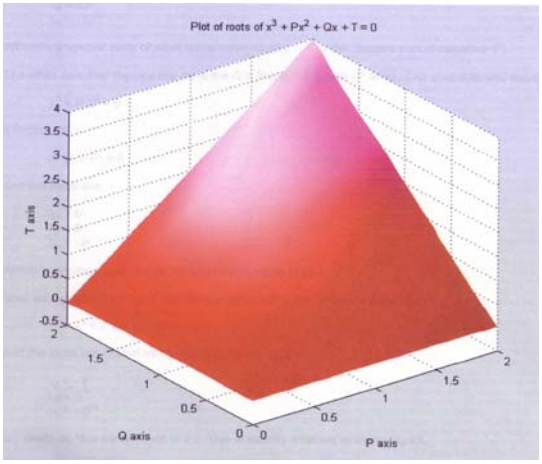

(b) Surface corresponds to Fig. 8: XY

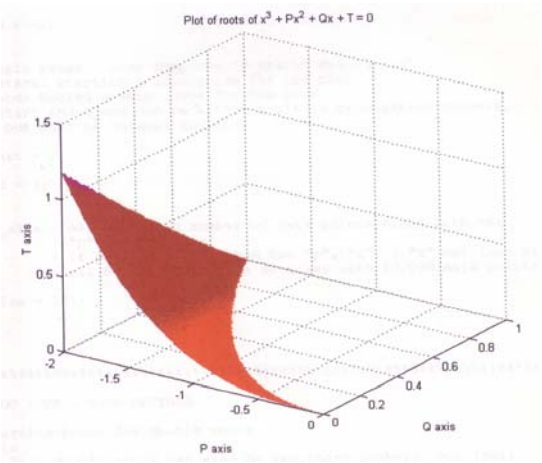

(c) Surface corresponds to Fig. 8: YZ

Fig. 9: P-Q-T surfaces for Fig. 2 transitions.

5. NDR REGION BIAS STABILITY

Single-valued bias in the NDR region requires that $R<|R_D|_{MIN}$, where $R_D<0$. The stability requirements for the 3rd order model of Brown et al are that $R>|R_D|$ from $T>0$, and $R<(L+L_Q)/|R_D|C$ from $Q>0$. The first conflicts with the bias condition, so stable NDR region bias is not possible with this model. For the 2nd and 4th order models, and for the 3rd order approximation to the 4th order one, the conditions are:

$$R < |R_D| \quad \& \quad R > (L+L_Q)/|R_D|(C_D+C_W),$$

where $(L+L_Q)$ and (C_D+C_W) reduce to L and C for the 2nd order, and L=0 for the 4th order approximation.

It is difficult to find reliable component data to test the models. Table 1 uses reference [2] data drawn from Gering [1] and Brown [3]. R_S is estimated from semiconductor parameters in both cases, but the stable plot of Figure 2C ("Gering C") suggests that the value of 0.17Ω is an underestimate. The table indicates that stable curve-tracing is also possible for "Brown 2 & 3," but the value of R_S=5Ω quoted does not meet the criteria. However, the most significant result is that there are RTD device structures for which stable curve-tracing will not be possible, even with zero stray circuit inductance. While, in comparison with TDs, L is typically one order of magnitude less, C may be 1-3 orders less, making the second requirement impossible to meet in some cases.

	High Frequency Measurements				Calculated		Charac	Stability			
RTD	R_S	C	L(nH)	R_D(Ω)	R_S(Ω)	C(pF)	$\|R_D\|_{MIN}$	$\|R_D\|$ > R > L/$\|R_D\|$C			Possible?
Gering A		3.00pF	1.01[1]	-2.0	<0.17	2.96		2.0Ω	0.17Ω?	168Ω	No
Gering B		2.75pF	0.93[1]	-5.7	<0.17	2.77		5.7Ω	0.17Ω?	59Ω	No
Gering C		2.60pF	0.89[1]	-156	<0.17	2.61		156Ω	0.17Ω?	2.2Ω	Yes[3]
Brown 1	5Ω	0.77fF					-33Ω	33Ω	5Ω	78Ω[2]	No
Brown 2	5Ω	18.5fF					-17Ω	17Ω	5Ω	5.9Ω[2]	Yes[4]
Brown 3	5Ω	2.8pf?					-50Ω	50Ω	5Ω	32Ω[2]	Yes[4]
Brown 4	5Ω	190fF?					-39Ω	39Ω	5Ω	14Ω[2]	Yes[4]

Table 1. Device and circuit parameters for negative differential resistance (NDR) region bias stability.

Notes:
(1) Lead inductance calculated to be 0.445nH
(2) Calculated from $L_Q=\tau_1|R_D|$, where $\tau_1= h/2\pi\Gamma_1$ and Γ_1 is resonant energy level half-width.
τ_1 lifetimes are 6.0ps (L_Q=19.8pH), 0.11ps (L_Q=1.87pH), 90ps (L_Q=4.5nH), 2.64ps (L_Q=88.44pH)
(3) Stable characteristic curve suggests R >2.2Ω
(4) 5Ω does not meet the second criterion for any case; (close for Brown 2)

REFERENCES

[1] J. M. Gering, D. A. Krim, D. G. Morgan, P. D. Coleman, W. Kopp, and H. Morkoc, "A small signal equivalent-circuit model for GaAs-$Al_xGa_{1-x}As$ resonant tunneling heterostructures at microwave frequencies", J. Appl. Phys., vol. 61, no. 1, 1987, pp. 271-276.

[2] C.-Y. Huang, J. E. Morris, and Y.-K. Su, "Generalized formula for the stability and instbility criteria of surrent-voltage characteristics measurements in the negative differential conductance region of a resonant tunneling diode", J. Appl. Phys., vol. 82, no. 5, 1997, pp. 2690-2696.

[3] E. R. Brown, C. D. Parker, and T. C. L. G. Sollner, "Effect of quasibound-state lifetime on the oscillation power of resonant tunneling diodes", Appl. Phys. Lett., vol. 54, no. 10, 1989, pp. 934-936.

[4] J. E. Morris, "Inductive effects in tunnel diode circuits," M.Sc. thesis, University of Auckland, 1967.